

# Mechanically Activated Combustion Synthesis of B<sub>4</sub>C-TiB<sub>2</sub> Nanocomposite Powder

Maryam Shojaie Bahaabad<sup>1\*</sup>

<sup>1</sup>Associated Professor, Department of Chemical and Material Engineering, Shahrood University of Technology, Shahrood, Iran

---

## ARTICLE INFO

### Article history:

Received 10 October 2016  
Accepted 28 December 2016  
Available online 15 March 2017

### Keywords:

Combustion synthesis  
Milling  
Boron carbide  
Titanium  
Diboride  
Nanocomposite

---

## ABSTRACT

In this study, in situ synthesis of B<sub>4</sub>C-TiB<sub>2</sub> nanocomposite powder was performed by mechanically activated combustion synthesis method. The molar ratio of B<sub>2</sub>O<sub>3</sub>:TiO<sub>2</sub>:Mg:C was 3:1:12:1 to obtain the B<sub>4</sub>C-TiB<sub>2</sub> nanocomposite. The milling process was used to mechanically activate the raw materials. Synthesis of prepared samples occurred in a furnace under argon atmosphere at 900 °C. The milling parameters were examined to optimize the activating process of the raw materials. The specimens were studied in various steps by XRD analysis for evaluation of phase compositions. Initially, the synthesized samples contained MgO, B<sub>4</sub>C, TiB<sub>2</sub> and a small amount of magnesium borates. XRD analysis after acid leaching of the combustion products showed a great effect of acid leaching on removing the impurities. It was demonstrated that mechanical activation is a useful method for simultaneous obtaining of B<sub>4</sub>C and TiB<sub>2</sub> powders. Morphology of the synthesized products was investigated by scanning and transmission electron microscopies (SEM & TEM). The final products were synthesized with a homogeneous morphology. The SEM analysis showed that the sample with 12 h of milling is made up of more uniform grains with smaller particle sizes (< 100 nm) than the sample with 6 h of milling.

---

## 1-Introduction

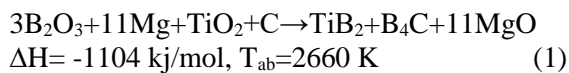
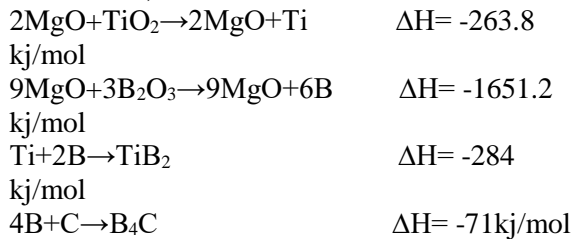
Boron carbide due to the combination of its remarkable hardness, high melting temperature (~2743 K), low density (2.52 g cm<sup>-3</sup>), wear resistance, chemical stability, neutron absorption capability, etc. is used in cutting tools, nuclear industry, military tools and thermoelectric applications [1-6]. However, due to the fragility and low sinterability of B<sub>4</sub>C, this compound should be composed with other materials. Due to its noticeable properties such as low density (4.52 g/cm<sup>3</sup>), high hardness (~25–35 GPa), high melting point (3230°C),

and high elastic modulus (~500 GPa), TiB<sub>2</sub> is an interesting compound for various structural applications [6]. B<sub>4</sub>C-TiB<sub>2</sub> composites can improve the sinterability and the special properties of the two compounds [7-10]. B<sub>4</sub>C-TiB<sub>2</sub> composites have remarkable properties such as strength, wear resistance and fracture toughness [11-15]. Therefore, these composites are very attractive materials in several industrial fields [16]. Few papers have been published about the synthesis of B<sub>4</sub>C-TiB<sub>2</sub> nanocomposite powder. Pei et al. [17] reported the synthesis of this composite powder via carbothermal

---

\* Corresponding author:  
E-mail: Mshojaieb@shahroodut.ac.ir

reduction. Halverson et al. [18] and Nikzad et al. [19] investigated the synthesis of B<sub>4</sub>C-TiB<sub>2</sub> nanocomposite powder via the combustion method by the use of B, C, and Ti powders. According to our research, there are not any paper about combustion synthesis of this nanocomposite powder via micropyretic process or metal oxides as raw materials. As such, in this study, synthesis of B<sub>4</sub>C-TiB<sub>2</sub> nanocomposite powder via metal oxides is investigated. The stoichiometric reaction of B<sub>4</sub>C-TiB<sub>2</sub> composites is as follow;



This reaction is exothermically suitable for combustion process. It is not easy to produce nanomaterials by combustion process because the particle size of the reactants is usually in the range of 10-100  $\mu\text{m}$  and combustion temperature is high ( $\geq 2000 \text{ K}$ ). So, mechanical activation as a promoter of SHS has been proposed for synthesis of nanostructured materials by combustion synthesis [20, 21]. The use of mechanical activation as a promoter of SHS also results in the formation of nanostructured materials. Mechanical activation reduces the particle size of the reactants and produces defects in their surface. Hence, the energy of the system increases and causes the reaction to be carried out at lower ignition temperature [22-26]. It should be mentioned that during combustion, in some systems, impurities or some undesirable compounds are produced. Acid leaching has been done to remove such impurities and undesirable compound. In many works, in order to remove MgO and other undesirable products, acid (HCl) leaching was used at different concentrations and times [4, 5, 8, 27]. In the present work, the effect of mechanical activation of the initial powders on the combustion synthesis of B<sub>4</sub>C-TiB<sub>2</sub> nanocomposite powder was investigated.

## 2-Experimental Procedure

### 2-1- Sample preparation

B<sub>2</sub>O<sub>3</sub> (Merck Art: 100 163), graphite (Merck Art: 104206,  $d_{50} < 50 \mu\text{m}$ , 99.5% purity), Mg metal (Merck Art: 818506,  $< 100 \mu\text{m}$ ) and TiO<sub>2</sub> (S.D. Fine Art: 40446,  $< 44 \mu\text{m}$ , 98% purity) powders were used as the starting materials. The proposed chemical reaction was represented in Eq. (1). Because of the evaporation of magnesium during combustion, the use of more than molar ratio of Mg to B<sub>2</sub>O<sub>3</sub> was suggested [5, 28]. Therefore, the molar ratio of Mg/B<sub>2</sub>O<sub>3</sub> was increased from 11/3 to 12/3. The molar ratio of B<sub>2</sub>O<sub>3</sub>: MgO: TiO<sub>2</sub>: C was 3:1:12:1 to obtain boron carbide and titanium diboride.

A self-propagating reaction easily occurs because of the highly exothermic nature of this reaction. The particle size of the powders produced by high exothermic reactions may be large; therefore, mechanical activation was used to reduce the size of the particles to nano-scale. High energy ball milling was carried out in 250 ml stainless steel container containing stainless steel balls at 200 rpm with 10:1 ball to powder ratio for 1, 3, 6, 12 and 24 h (denoted as BTO1, BTO3, BTO6, BTO12 and BTO24) under argon atmosphere. The milled powders were compacted by a uniaxial press with 13 mm diameter and 10 mm height at 300 MPa. The combustion reactions were carried out in a tubular furnace under a continuous argon gas flow at 900°C. The combustion temperature was measured by laser pyrometer, which was focused on the surface of some of the samples. After combustion, MgO and unwanted products were removed by leaching in hot hydrochloric acid (10 wt%) for 1 h. The leached products were dried in an oven at 333 K for 24 h.

### 2-2- Characterization

The particle size of the leached samples was measured by particle size analyzer (Fritsch Analysette German). Thermal analysis was done by DTA-TG under argon gas at the heating rate of 30 K/min. The phase compositions of samples were determined by X-ray diffraction (Philips PW 3710) using Cu-k $\alpha$  radiation ( $\lambda = 0.154 \text{ nm}$ ) after each of the three steps of milling, synthesis, and leaching. Morphology of the leached synthesized powders was characterized by scanning electron microscopy (SEM, Stereo Scan S360) and transmission electron microscopy

(TEM, FEG Philips CM200). At first, a small amount of the powder was dispersed in distilled water using an ultrasonic bath. Then, a small drop of suspension was put on the center of the carbon film using a micro pipet and dried at ambient temperature for 30 min.

### 3-Results and Discussion

The reaction of  $B_2O_3$  reduction by Mg and the formation of  $B_4C$ - $TiB_2$  composites (Eq. (1)) have an appropriate adiabatic temperature about 2660 K calculated by Eq (2) [29].

$$\Delta H_r^{\circ} = \int_{298K}^{T_{rd}} \sum n C_p(\text{products}) dT \quad (2)$$

Figure 1 shows the X-ray diffraction patterns of the mixed and milled powders for different milling times. The pattern of the starting powder mixture (BTO) showed all of the expected peaks of Mg,  $TiO_2$ ,  $B_2O_3$ , and graphite. The low intensity of  $B_2O_3$  and graphite peaks in the XRD pattern is related to the low mass absorption coefficient in comparison with Mg and Si. After 1 h, the intensity of the C and  $B_2O_3$  peaks decreased while

the peaks for Mg and  $TiO_2$  phases remained unchanged. No new phases were formed during milling from 3 to 12 h except for Mg. All of the peaks of reactants disappeared and  $Ti_3O_5$  was formed after 24 h. This means that the reaction had occurred and the products were formed. Figure 2 shows the particle sizes of the reactants after milling. It can be seen that the particle sizes decreased as the milling time increased. The mean particle size of the reactants milled for 1 h was 52  $\mu m$  and decreased to 27  $\mu m$  after 12 h of milling.

Typical DTA/TG data from the mixed powders ( $B_2O_3$ , Mg,  $TiO_2$  and C) milled for 1 h (BTO1) and 12 h (BTO12) are shown in Figure 3. The first endothermic peak at 150  $^{\circ}C$  corresponds to dehydration of  $B_2O_3$  and the second endothermic peak at about 654 $^{\circ}C$  corresponds to the melting of Mg. The first exothermic peak at 632 $^{\circ}C$  corresponds to the reduction of  $TiO_2$ . The second exothermic peak at 765 $^{\circ}C$  reflects the crystallization of  $TiB_2$  and  $B_4C$ . These results were also confirmed by Weimin et al. [30] during DTA analysis of the mixture of  $B_2O_3$ ,  $TiO_2$  and Mg.

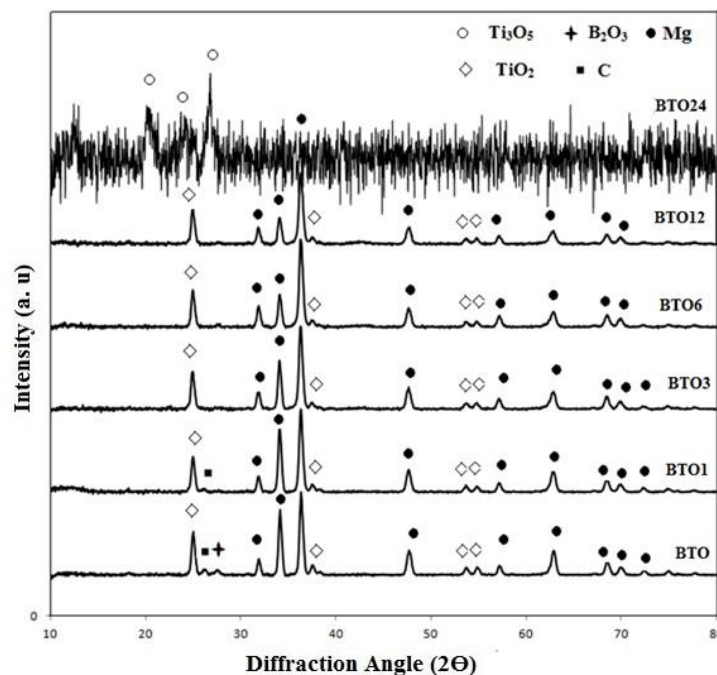


Fig. 1. XRD patterns of the milled samples.

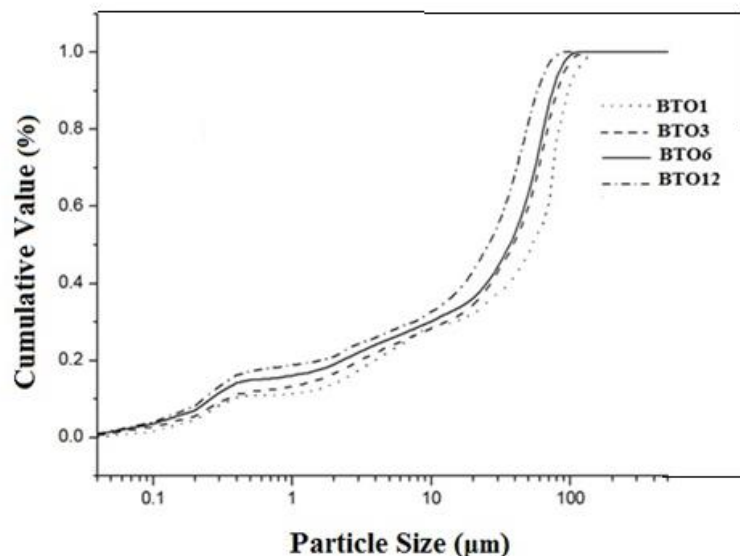


Fig. 2. Effect of milling on the particle sizes of the reactants.

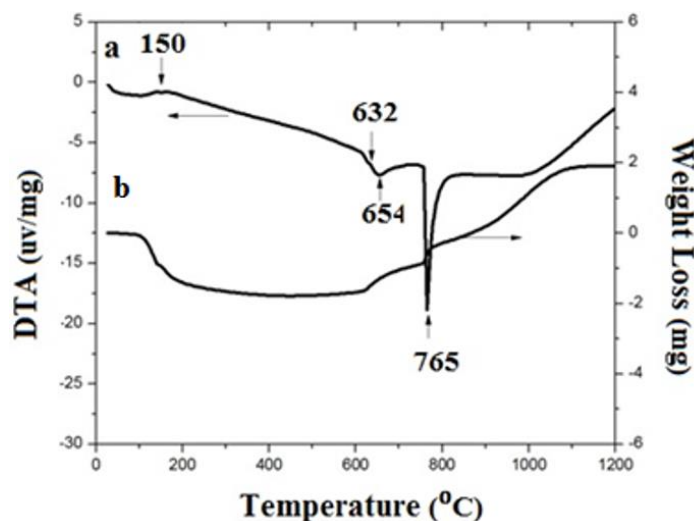


Fig. 3. TG/DTA plots of the mixed powders a) milled for 1h, b) milled for 12 h under argon atmosphere at the heating rate of 30K/min.

DTA results imply that the ignition temperature is more than 700°C. Therefore, the combustion process was done at 900°C. The comparison of DTA results for BTO1 and BTO12 reveals that all peaks for BTO12 shifted to higher temperatures and the intensity of the main exothermic peak decreased. This may be attributed to the formation of phases that cannot be detected by XRD. These phases can act as a diluent and change the thermodynamic parameters (ignition temperature, adiabatic temperature, etc.).

During combustion, magnesium plays an important role as a reducing agent. The

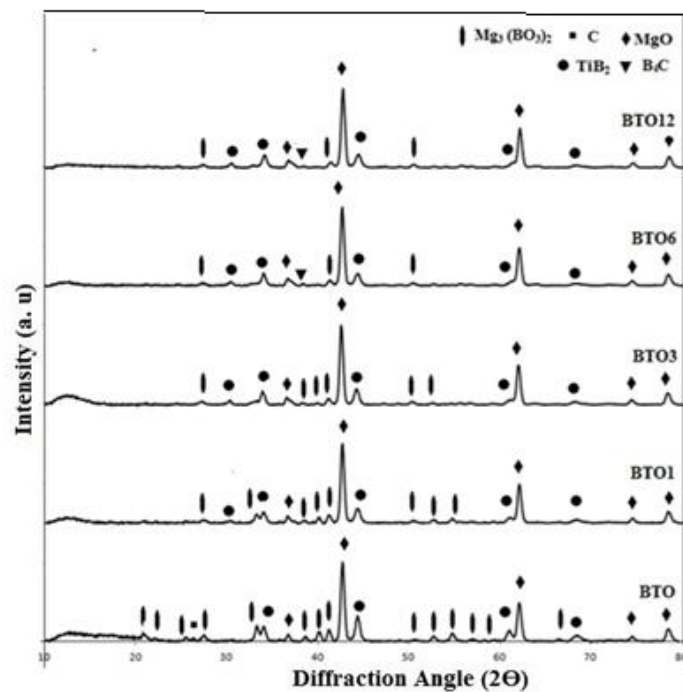
combustion reaction was accompanied by vaporization of magnesium because of its low boiling point. Thus, there was a white gas in the furnace for all samples. Therefore, the samples may be broken up, especially those prepared from powders milled for more than 3 h. The combustion time was recorded by measuring the period of time required to place the samples into the furnace and complete the reactions. It can be seen in Figure 2 that the particle sizes decreased by increasing the milling time. Thus, the combustion time and the combustion temperature decreased (Table 1).

**Table 1.** The combustion temperature and the time of reactions.

Sample	Average Combustion Temperature (°C)	Combustion Time (S)
BTO	1631	84
BTO1	1834	72
BTO3	1734	58
BTO6	1781	47
BTO12	1664	20

Figure 4 shows the XRD patterns of the samples after the combustion reaction. MgO was major phase in all of the combusted samples which was also confirmed by Eq. (1). SiC phase could be seen but B<sub>4</sub>C phase could not be detected due to the low intensity and overlapping of the peaks with other higher intensity compounds. Also, magnesium borates (Mg<sub>2</sub>B<sub>2</sub>O<sub>5</sub> and Mg<sub>3</sub>B<sub>2</sub>O<sub>6</sub>) were detected. Production of Mg<sub>2</sub>B<sub>2</sub>O<sub>5</sub> and Mg<sub>3</sub>B<sub>2</sub>O<sub>6</sub> is due to the Mg evaporation in the

furnace during the combustion reaction that leads to the remaining of some unreduced B<sub>2</sub>O<sub>3</sub> and then the formation of magnesium borates from synthesized MgO and remaining B<sub>2</sub>O<sub>3</sub> [5, 20]. It is worth mentioning that the formation of Mg<sub>2</sub>B<sub>2</sub>O<sub>5</sub> and Mg<sub>3</sub>B<sub>2</sub>O<sub>6</sub> decreased by decreasing the particle size of Mg. The formation of magnesium borate decreased because of more complete reduction reaction of B<sub>2</sub>O<sub>3</sub> with Mg. Figure 5 shows the XRD patterns of the synthesized samples after acid leaching.

**Fig. 4.** XRD patterns of the powders mixture after combustion synthesis..

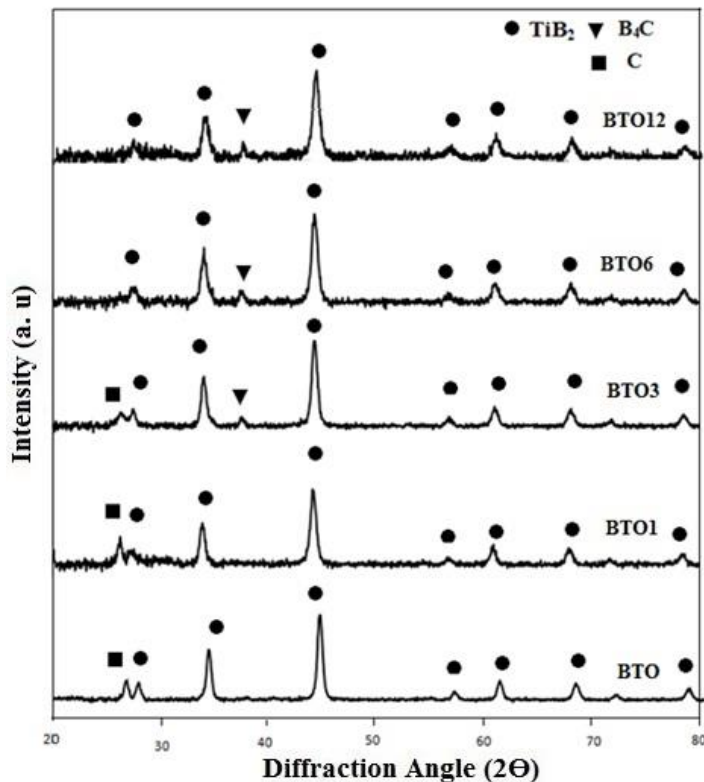
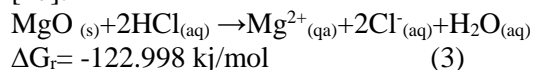


Fig. 5. XRD patterns of the combustion product after acid leaching.

These patterns confirm that acid leaching was successfully carried out for elimination of magnesium oxide and undesirable products. This confirms that the peaks of undesirable products belong to  $Mg_3B_2O_6$  and  $Mg_2B_2O_5$ . Eq. (3) is considered for elimination of magnesium oxide [27].



In the case of the elimination of magnesium borates, it seems that these compounds have been decomposed to boron oxide and magnesium oxide in acidic solution while according to Eq. (3), MgO has been dissolved and boron oxide has remained in the amorphous state [31, 32].

Figure 6 shows the SEM micrograph of the samples after acid leaching. It can be seen that the agglomerated particles were composed of rough and circular fine particles with sub-micron up to 250 nm sizes. It seems that the formation of  $B_4C$  and SiC in a net of MgO and with a high velocity

of reaction has caused an increase in nucleation and prevention of grain growth. In Eq. (1), at first Mg reduces  $B_2O_3$  and then the formation of  $B_4C$  and SiC occurs due to the heat of the reduction reaction.

TEM images of the BTO6 and BTO12 samples after acid leaching (Figure 7) shows that the particles are composed of grains with a maximum size of 40 nm. Uniformity of the size and shape of the grains can be well clearly seen in TEM images, which confirm the mechanically activated compustion method is successful to synthesize  $B_4C$ - $TiB_2$  nanocomposite with appropriate morphology. The TEM analysis shows the sample with 12 h of milling of the raw materials is composed of more uniform grains than the sample with 6 h of milling of the raw materials. In Figure 3c-d, the SAED patterns of the powders shows spotty ring patterns without any additional diffraction spots, revealing that the particle size of  $B_4C$ - $TiB_2$  powder is nano-scale.

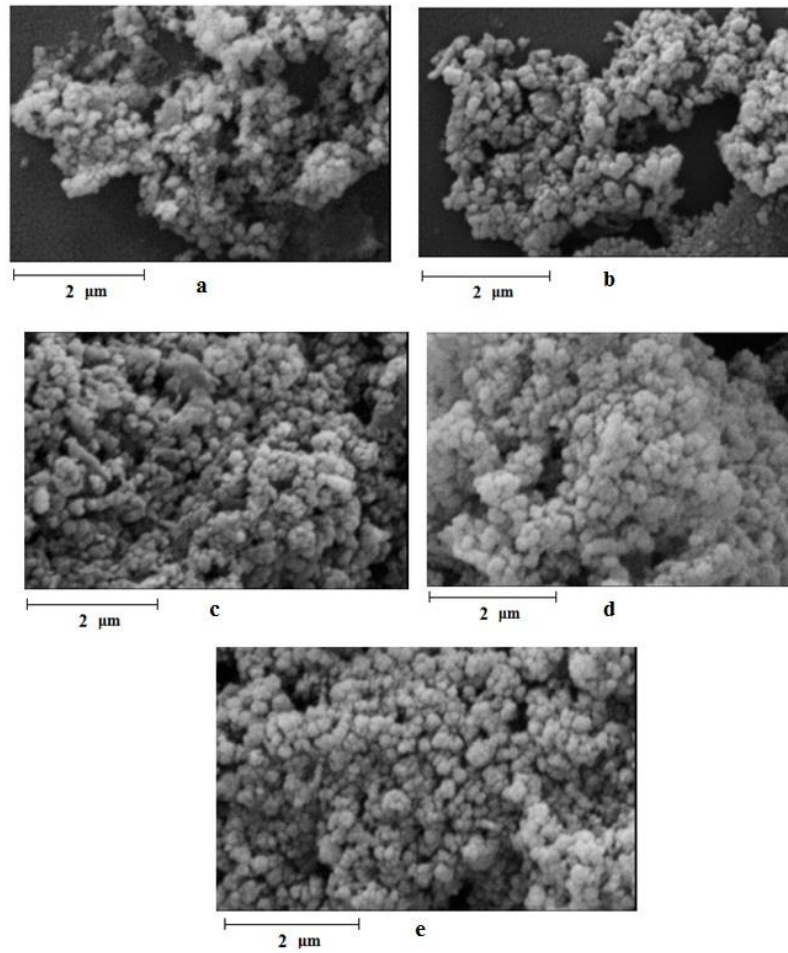


**Fig. 6.** SEM image of the leached samples a) BTO, b) BTO1, c) BTO3, d) BTO6 and e) BTO12.

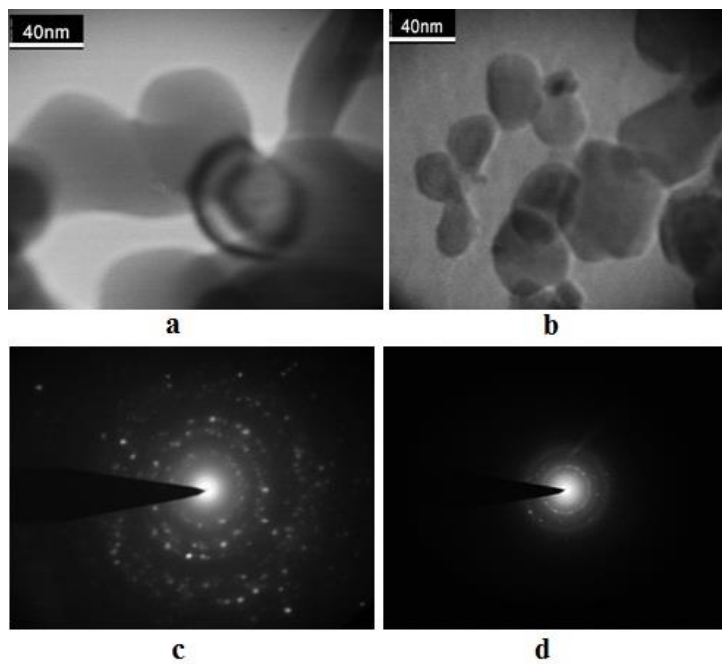


**Fig. 7.** TEM image of the leached samples a) BTO6, b) BTO12, c) SAED of BTO6, d) SAED of BTO12.

#### 4-Conclusion

B<sub>4</sub>C-TiB<sub>2</sub> nanocomposite powder was successfully synthesized by mechanically activated combustion synthesis (MACS) method. The XRD patterns confirmed that increasing the milling time leads to the decrease of the formation of magnesium borates. Also, acid leaching by HCl solution was successful to remove unfavorable compounds and purify the products. SEM analysis confirmed the formation of particles in nanometric scale for all samples. TEM analysis revealed that BTO12 with 12 h of milling compared to BTO6 with 6 h of milling is composed of grains with more uniformity and smaller size.

#### References

[1] F. Thevenot, "Boron carbide: Comprehensive review", *J. Eur. Ceram. Soc.*, Vol. 6, 1990, pp. 205-225.

[2] H. Nishikawa, "Powder or boron compound at present", *Ceramics*, Vol. 22, 1987, pp. 40-45.

[3] K. Takagi, "Boride materials", *Met. Technol.*, Vol. 1, 1993, pp. 23-28.

[4] F. Deng, H.Y. Xie, L. Wang, "Synthesis of submicron B<sub>4</sub>C by mechanochemical method", *Mater. Lett.*, Vol. 60, 2006, pp. 1771-1773.

[5] L. Nikzad, T. Ebadzadeh, M.R. Vaezi, A. Tayebifard, "Effect of milling on the combustion synthesis of ternary system B<sub>2</sub>O<sub>3</sub>, Mg and C", *Micro. Nano. Lett.*, Vol. 7, 2012, pp. 366-369.

[6] E. Mohammad Sharifi, F. Karimzadeh, M.H. Enayati, "Mechanochemical assisted synthesis of B<sub>4</sub>C nanoparticles", *Adv. Powder. Technol.*, Vol. 22, 2011, pp. 354-358.

[7] G. Liu, J. Li, Y. Shan, J. Xu, "Highly dense b-SiC ceramics with submicron grains prepared by sintering of nanocrystalline powders", *Scr. Mater.*, Vol. 67, 2012, pp. 416-419.

[8] Z. Zhang, X. Du, W. Wang, Z. Fu, H. Wang, "Preparation of B<sub>4</sub>CeSiC composite ceramics through hot pressing assisted by mechanical alloying", *Int. J. Refract. Metals. Hard. Mater.*, Vol. 41, 2013, pp. 270-275.

[9] F.C. Sahin, B. Apak, I. Akin, H.E. Kanbur, D.H. Genckan, A. Turan, G. Goller, O. Yucel, "Spark plasma sintering of B<sub>4</sub>CeSiC

composites", *Solid. State. Sci.*, Vol. 14, 2012, pp. 1660-1663.

[10] A. Li, Y. Zhen, Q. Yin, L. Ma, Y. Yin, "Microstructure and properties of (SiC, TiB<sub>2</sub>)/B<sub>4</sub>C composites by reaction hot pressing", *Ceram. Int.*, Vol. 32, 2006, pp. 849-856.

[11] D.K. Kim, C.H. Kim, "Pressureless sintering and microstructural development of B<sub>4</sub>C-TiB<sub>2</sub> based composites", *Adv. Ceram. Mater.*, Vol. 3, 1988, pp. 52-55.

[12] S. Tuffe, J. Dubois, G. Fantozzi, G. Barbier, "Densification, microstructure and mechanical properties of TiB<sub>2</sub>-B<sub>4</sub>C based composites", *Int. J. Refract. Met. Hard. Mater.*, Vol. 14, 1996, pp. 305-310.

[13] R.G. Munro, "Material Properties of Titanium Diboride", *J. Res. Natl. Ins. Stan. Tech.*, Vol. 105 2000, pp. 709-720.

[14] V. Skorokhod, M.D. Vlajic, V.D. Krstic, "Mechanical properties of pressureless Sintered boron carbide containing TiB<sub>2</sub> phase", *J. Mater. Sci. Lett.*, Vol. 15, 1996, pp. 1337-1339.

[15] V. Skorokhod, V.D. Krstic, "High strength-high toughness B<sub>4</sub>C-TiB<sub>2</sub> composites", *J. Mater. Sci. Lett.*, Vol. 19, 2000, pp. 237-239.

[16] S. Yamada, K. Hirao, Y. Yamauchi, S. Kanzak, "High strength B<sub>4</sub>C-TiB<sub>2</sub> composites fabricated by reaction hot-pressing", *J. Eur. Ceram. Soc.*, Vol. 23, 2003, pp. 1123-1130.

[17] L.Z. Pei, H.N. Xiao, "B<sub>4</sub>C/TiB<sub>2</sub> Composite powders prepared by carbothermal reduction method", *J. Mater. Process. Tech.*, Vol. 209, 2009, pp. 2122-2127.

[18] D.C. Halverson, B.Y. Lum, Z.m A. Munir, "Combustion Synthesis of Boride and Other Component", US Patent No. 4879262, 1989.

[19] L. Nikzad, R. Licheri, M.m,R. Vaezi, R. Orrù and G. Cao, "Chemically and mechanically activated combustion synthesis of B<sub>4</sub>C-TiB<sub>2</sub> composites", *Int. J. Refract. Met. Hard. Mater.*, Vol. 35, 2012, pp. 41-48.

[20] S.T. Aruna, A.S. Mukasyan, "Combustion synthesis and nano materials", *Curr. Opin. Solid. State. Mater. Sci.*, Vol. 12, 2008, pp. 44-50.

[21] P. Mossino, "Some aspect in self propagation high temperature synthesis", *Ceram. Int.*, Vol. 30, 2004, pp. 311-332.

[22] H.B. Jin, J.T. Li, M.S. Cao, S. Agathopoulos, "Influence of mechanical activation on combustion synthesis of fine silicon carbide (SiC)

powder”, *Powder. Technol.*, Vol. 196, 2009, pp. 229–232.

[23] J.J. Moore, H.J. Feng, “Combustion synthesis of advanced materials: Part I. Reaction parameters”, *Prog. Mater. Sci.*, Vol. 39, 1995, pp. 243–273.

[24] S.T. Aruna, A.S. Mukasyan, “Combustion synthesis and nanomaterials”, *Curr. Opin. Solid State Mater. Sci.*, Vol. 12, 2008, pp. 44–50.

[25] L. Takacs, “Self-sustaining reactions induced by ball milling”, *Prog. Mater. Sci.*, Vol. 47, 2002, pp. 355–414.

[26] P. Mossino, “Some aspects in self-propagating high-temperature synthesis”, *Ceram. Int.*, Vol.30, 2004, pp. 311–332.

[27] U. Demircan, B. Derin, O. Yücel, “Effect of HCl concentration on TiB<sub>2</sub> separation from a self-propagating high-temperature synthesis (SHS) product”, *Mater. Res. Bull.*, Vol. 42, 2007, pp. 312-318,

[28] M. Alkan, M.S. Sonmez, B. Derin, O. Yücel, “Effect of initial composition on boron carbide production by SHS process followed by acid leaching”, *Solid. State. Sci.*, Vol.14, 2012, pp. 1688-1691.

[29] H. Roghani, “Effect of milling parameters on the phase transformations and morphology changes of B<sub>4</sub>C-SiC nanocomposite powder in situ synthesized by MAVCS method”, *J. Ceram. Pro. Res.*, Vol. 17, 2016, pp. 170-175.

[30] W. Weimin, F. Zhengyi, W. Hao, Y. Runzhang, “Chemistry reaction processes during combustion Synthesis of B<sub>2</sub>O<sub>3</sub>-TiO<sub>2</sub>-Mg system”, *J. Mater. Process. Tech.*, Vol. 128, 2002, pp. 162–168.

[31] J.D. Makinson, J.S. Lee, S.H. Magner, R.J.D. Angelis, W.N. Weins, A.S.Hieronimus, “X-ray diffraction signatures of defects in nanocrystalline materials”, *Int. Cent. Diffraction Data.*, Vol. 42, 1998, pp. 5-9.

[32] Y. Zhao, J. Zhang, “Microstrain and grain-size analysis from diffraction peak width and graphical derivation of high-pressure thermomechanics”, *J. Appl. Crystallogr.*, Vol. 41, 2001, pp. 1095–1108.